



Missouri State[™]
U N I V E R S I T Y

BearWorks

College of Natural and Applied Sciences

2-1-2006

Template-free synthesis of conducting-polymer polypyrrole micro/ nanostructures using electrochemistry

S. Gupta

Missouri State University

Follow this and additional works at: <https://bearworks.missouristate.edu/articles-cnas>

Recommended Citation

Gupta, S. "Template-free synthesis of conducting-polymer polypyrrole micro/nanostructures using electrochemistry." *Applied physics letters* 88, no. 6 (2006): 063108.

This article or document was made available through BearWorks, the institutional repository of Missouri State University. The work contained in it may be protected by copyright and require permission of the copyright holder for reuse or redistribution.

For more information, please contact bearworks@missouristate.edu.

Template-free synthesis of conducting-polymer polypyrrole micro/nanostructures using electrochemistry

S. Gupta^{a)}

Department of Physics, Astronomy, and Materials Science, Missouri State University, Springfield, Missouri 65897

(Received 23 September 2005; accepted 6 January 2006; published online 8 February 2006)

Controlled synthesis of conducting-polymer polypyrrole microcontainers by electrogenerated H₂ gas bubbles act as template from a surfactant *cum* electrolyte (2-naphthalene sulfonic acid; β -NSA) on a stainless steel working electrode, followed by the electrochemical polymerization of pyrrole around the micelles is reported. The films consist of round grains and cup/bowl-like structures, which became lantern-like with increasing cycles. Sodium chlorate (NaClO₃) was used as a reference electrolyte. The bowl diameter and room temperature conductivity ranged 50–2000 nm and 1–50 S cm⁻¹, respectively. An analysis of these films was complemented with Raman spectroscopy to identify the oxidized PPy, polaron, and bipolarons. © 2006 American Institute of Physics. [DOI: 10.1063/1.2168688]

Conjugated organic semiconducting materials (or conducting polymers) are currently experiencing the dawn of their commercialization in electroluminescent and photovoltaic devices.¹ Other potential applications include batteries, gas sensors, electrochromic devices, biomedical science (or drug delivery), nanoelectronics, supercapacitors, and light-weight compact actuators.² During the last almost three decades, there was an increasing interest in the study of materials with reduced dimensions (2D, 1D, and 0D) such as thin films, nanotubes or wires, and metallic clusters or nanoparticles, respectively. The large interest for these materials is due to the exceptional structural and physical properties that they can present compared to their bulk counterpart (3D). Several methods have been devised to synthesize polymer materials with low dimensionality: chemical or solution, plasma, and electrochemical polymerization. Martin *et al.*³ and others⁴ have used commercial membranes as templates to prepare a variety of nanoscale materials, and this method has been used successfully for various conducting polymers (polyacetylene, polyaniline, and polypyrrole). Furthermore, PPy nanowires have been synthesized by electrochemical polymerization with a scanning microneedle as an electrode.⁵ All these methods require a rather tedious post-deposition process for removal of the template to release the micro/nanostructured polymers.⁶

Recently, Shi *et al.*⁷ and others⁸ have reported the electrochemical deposition of template-free PPy microcontainers onto “soap bubbles” associated with O₂ released from an electrolysis of water (H₂O) in an aqueous solution of β -naphthalenesulfonic acid (β -NSA), which acts as both surfactant and electrolyte. The direct generation of O₂ gas on the working electrode under a relatively positive potential have a detrimental overoxidation effect, therefore we started the electrochemical polymerization of PPy by releasing H₂ (electrolysis of H₂O) around the working electrode under a negative potential (–1.0 to –1.4 V). The released H₂ gas bubbles were stabilized by the anionic surfactant molecules in the solution and assembled onto the working electrode

under a positive potential to act as the “soap bubble” template for the formation of micro/nanostructured conducting polymers. Unlike the previously reported “soap bubble” template synthesis produced no PPy microstructures at the potential below 0.9 V, the modified method allowed their formation at a rather low potential, as we shall see later. In this letter, we report use of the “soap-bubble” template synthesis for making polypyrrole micro- bowls/cups with controlled morphology and microscopic structures and gleam on our understanding of the bubble nucleation at the solid-electrolyte interface. We entitle this templateless approach as an effective utilization of bubbles: “*bubbology*.” Furthermore, in the family of π -conjugated polymers, PPy stands out and is chosen because of its high conductivity, air stability, and several advanced applications.⁹ The molecular structure using vibrational spectroscopy and room temperature electrical properties are discussed and correlated.

We have used electrochemical technique to polymerize pyrrole onto stainless steel substrates and the experimental details are described as follows. Pyrrole (99%) and β -NSA (2-naphthalenesulfonic acid, sodium salt 95%) were purchased from Alfa-AEsar and used as it is. The electropolymerization of pyrrole was carried out on Solartron 1287 electrochemical interface in a 5 mL single compartment three electrode electrolyte cell at room temperature, where we used two stainless steel sheets (3 cm × 0.3 cm × 0.6 mm) as the working and counter/auxiliary electrodes and a standard Ag/AgCl for reference. The sheets of stainless steel (Grade: SS321) substrates were hand polished and cleaned with acetone and deionized water several times. The working and counterelectrodes were placed 0.5 cm apart. The cell contained two different aqueous electrolytes: (i) 0.25 M pyrrole and 0.4 M NaClO₃ (sodium chlorate, 99% min and (ii) 0.25 M pyrrole and 0.4 M β -NSA. Prior to the electropolymerization, the electrolyte solution was degassed with a pure nitrogen flow. Cyclic voltammetry scan(s) were performed to generate H₂ bubbles on the working electrode surface by scanning the potential from –1.0 to –1.4 V for the first cycle, followed by changing the potential window to the range of 0.5 to 1.1 V for three subsequent cycles for electropolymerization of pyrrole around the “soap bubbles” on the working

^{a)} Author to whom correspondence should be addressed; electronic mail: SGupta@MissouriState.edu

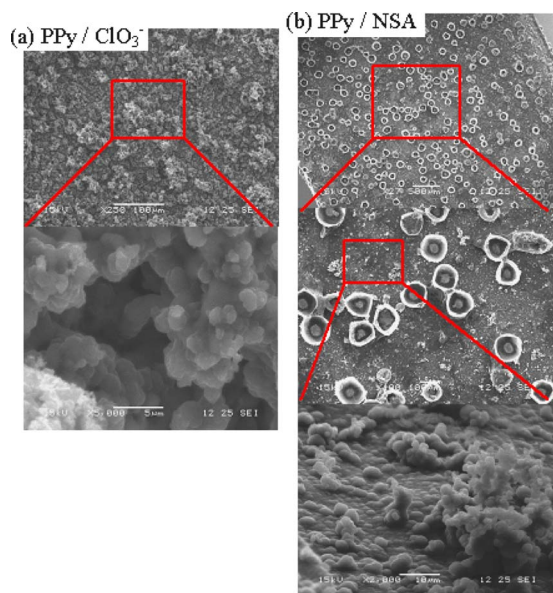


FIG. 1. (Color online) SEM images of the electrochemically synthesized conducting polymer polypyrrole using (a) NaClO_3 and (b) $\beta\text{-NSA}$ electrolytes displaying a significant difference in the surface structure. The cyclic voltammetric polymerization was over a 0.4 to 1.1 V potential window, scanning rate of 10 mV s^{-1} , 3 cycles. The aqueous electrolyte solutions contain 0.4 M NaClO_3 , 0.4 M $\beta\text{-NSA}$, and 0.25 M pyrrole (scale bars: 500, 100, and $10 \mu\text{m}$).

electrode at 10 mV s^{-1} . As a reference, conventional polypyrrole films were electropolymerized using sodium chlorate (rather perchlorate) for three cycles over the same potential window. Without the first cycle over a negative potential window, we observed no electropolymerization and no microstructure formation, indicating that the H_2 gas is responsible for the template-free syntheses.

The surface morphology of the films was revealed by scanning electron microscopy JEOL (JEOL Model 6400) with an acceleration voltage of 15 kV. Raman spectroscopy (RS) was used to analyze the structure and molecular bonding in the films. RS analyses were carried out using excitation wavelength of 514.5 nm ($E_L=2.41 \text{ eV}$) from an Ar^+ laser and a ISA J-Y TRIAX 320 spectrometer in a back-scattering geometry. All of the spectra were measured with a beam spot size of $\sim 3 \mu\text{m}$ with minimum power density ($\sim 10 \text{ kW/cm}^2$) to avoid thermal degradation. All of the Raman spectra were fitted using Jandel Scientific Peakfit software (v. 4.0) based on the Marquardt-Levenberg method. For the electrical resistivity measurements, a custom-built two-probe system composed of a Keithley 6517 programmable meter unit acts as both a voltage source and a current meter was used. These measurements permitted us to determine contact electrical resistance.

Figure 1 shows typical scanning electron micrographs revealing the morphology of as-deposited polypyrrole microstructures: $\text{PPy}/\text{ClO}_3^-$; Fig. 1(a) and PPy/NSA ; Fig. 1(b). The solution containing a monomer and $\beta\text{-NSA}$ looked like an emulsion due to the surfactant characteristics of the $\beta\text{-NSA}$ dopant. The results showed reasonable reproducibility. It is apparent that the morphology of PPy is significantly affected by the changes of the electrolyte. The former provided a conventional PPy film with crumpled grains, while an unusual morphology was observed with the latter. It is suggested that the $\beta\text{-NSA}$, which acts as an anionic surfactant, prevents coagulation and forms a uniform conventional film

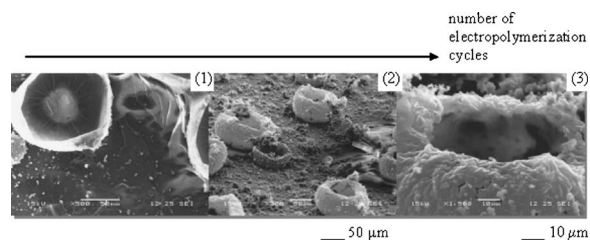


FIG. 2. SEM images of the electrochemically synthesized conducting polymer polypyrrole microstructures. The aqueous electrolyte solutions contain 0.4 M $\beta\text{-NSA}$ and 0.25 M pyrrole.

as in the case of $\text{PPy}/\text{ClO}_3^-$. It is also clear from the microstructures' images that they are upright on the electrode surface, have fairly good uniformity, and randomly align in a high density of about $2000\text{--}4000 \text{ units cm}^{-2}$. It was demonstrated that the noncorrosive stainless steel sheet is essential as a working electrode producing microcup/bowl or container-like morphology in contrast to ITO and HOPG substrates.¹⁰

The morphology of the PPy/NSA films other than the microbowls is also shown that looks like round grains with size ranging $2\text{--}5 \mu\text{m}$. The morphology of the microcups' changes as a function of the number of cyclic voltammetry scans, i.e., three cycles and they change their shape from microbowl- to microlantern-like. Their caliber also increases, ranging $50\text{--}70 \mu\text{m}$ (see Fig. 2). The walls of the microcups, which were smoother and semitransparent start to become complex with presence of material/residue around and on them and become thicker with increasing cycles. Although microcontainers with different sizes have been observed, the majority of them formed under this experimental condition have a bowl-like shape. Figure 3 shows three-dimensional atomic force microscopy images of the films in a $10 \times 10 \mu\text{m}^2$ scan size. It is clear that the surfaces of the $\text{PPy}/\text{ClO}_3^-$ are relatively smoother and less featured, unlike PPy/NSA and corresponding surface roughness (σ_{rms}), is ~ 0.52 and $0.68 \mu\text{m}$, respectively.

Concerning formation mechanism, the question is what induces the unusual growth of PPy microstructures on the electrode surface? It is reasonable to assume that the "soap bubble" or electrogenerated H_2 "gas bubble" in conjunction with these micelles play a template-like role. Furthermore, the onset oxidation potential from the polarization curve of the electrolyte at a PPy film with a microcups-coated SS electrode was found to be $\sim ca. 0.80 \text{ V}$ in contrast to $ca. 0.9 \text{ V}$ for NaClO_3 , which implied that the PPy film can catalyze the decomposition of water. The decrease in potential value should not be overlooked. It was found that by changing the

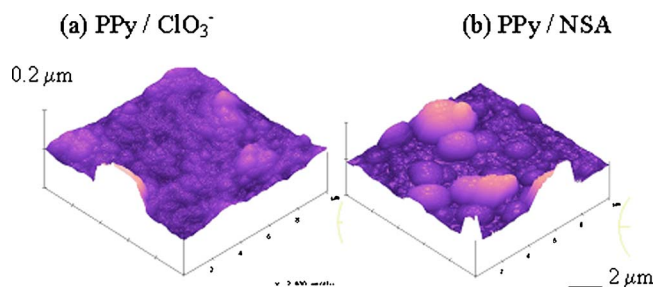


FIG. 3. (Color online) Shown are three-dimensional atomic force microscopy images over $10 \times 10 \mu\text{m}^2$ for the (a) $\text{PPy}/\text{ClO}_3^-$ and (b) PPy/NSA films.

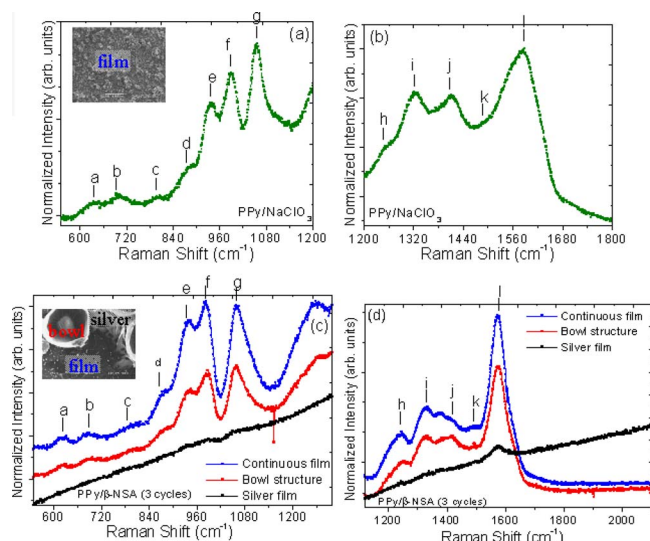


FIG. 4. (Color online) Representative visible micro-Raman spectra excited at 514.5 nm of (a), (b) PPy/ ClO_3^- and (c), (d) PPy/NSA in (left) low- and (right) high-frequency regions. The inset shows images of the films where the Raman spectra were taken.

electropolymerization condition (scan rate, electrolyte concentration, number of cycles, potential window) different shapes, sizes, caliber of polypyrrole microstructures can be generated that have potential applications. For instance, these microstructures may be used as a biological microencapsulation substance.^{8,11}

Raman spectroscopy (RS) is proved to be an invaluable nondestructive characterization tool to probe structural bonding in conjugate polymer films. The high sensitivity of visible radiation ($\lambda_L=514.5$ nm to the π states, the bands are resonantly enhanced. Figure 4 displays resonance Raman spectra in the low ($600\text{--}1200$ cm^{-1}) and high-frequency ($1200\text{--}2000$ cm^{-1}) regions for both the representative polypyrrole films synthesized for three cycles. For a realistic comparison, the spectra were normalized with respect to the intense high-frequency band. The Raman spectra were taken at three different places for PPy/NSA films: continuous film, bowl structure, and silvery film, as indicated in Fig. 4(c). The Raman bands are assigned following Ref. 12. It is clear that the Raman spectra of continuous film and the bowl structure are similar and silvery area does not show any important features. Qualitatively speaking, the Raman spectra from PPy/ ClO_3^- and PPy/NSA differ in some of the Raman signatures and peak positions. This is because Raman spectra of doped polypyrrole have provided evidence for the existence of polarons (radical cations) and bipolarons (dictations), which act as charge carriers and are considered to be localized structural defects associated with a conjugated carbon backbone.¹³ The relatively broad bandshapes suggest a partial disordered structure with short conjugation sequences. Prominent bands depicted in Fig. 4 from (a)–(l) are (a) 615 cm^{-1} (ring torsional); (b) 712 cm^{-1} (C–H wagging); (c) 826 cm^{-1} (C–H wagging); (d) 880 cm^{-1} (ring deformation); (e) 937 cm^{-1} (ring deformation associated with dictation); (f) 970 cm^{-1} (ring in-plane deformation associated with radical cation); (g) 1070 cm^{-1} (symmetrical C–H in-plane bending and N–H in-plane deformation associated with a radical cation, i.e., of the oxidized (doped) species, including ClO_3^- doping, a naphthalene ring, and a– SO_3^- group of dopant); (h)

1236 cm^{-1} (antisymmetrical C–H in-plane bending); (i) 1320 cm^{-1} (“reasonably” C–C in-ring and C–C inter-ring stretching); 1370 cm^{-1} (present as a doublet in PPy/NSA film and absent in PPy/ ClO_3^- antisymmetrical in-ring C–N stretching); (j) 1410 cm^{-1} (C–C and C–N stretching); (k) 1500 cm^{-1} weak band—absent in PPy/ ClO_3^- and present in PPy/NSA (skeletal band; C–C and C–N stretching); and (l) 1590 cm^{-1} (C=C in-ring and C–C inter-ring stretching, which is an overlap of bands arising due to a radical cation and dictation) represents the backbone. The corresponding band of a neutral species at 1050 cm^{-1} is relatively weak. In addition, the ratio between the intensity of the l (oxidization state sensitive) to k (skeletal band) band determines the chain or, more appropriately, relative conjugation length, which comes out to be 1.2 and 1.5 for PPy/ ClO_3^- and PPy/NSA films, respectively. This effect is well marked for PPy/ ClO_3^- round grains.

The variation of the electrical resistance is largely on discussion for their effective utilization in molecular electronics. The room temperature electrical measurements (current-voltage) in a two-terminal configuration provide us a measure of contact resistance for PPy/NSA and PPy/ ClO_3^- films to be 30 and 170 $\text{k}\Omega$, respectively. We must note that the increase of the C=C stretching band versus the intensity of the skeletal band implies that the polarizability of the system is higher for narrower PPy microcontainers, which is also in direct correspondence with the increase in conductivity.

In summary, we have demonstrated that surfactant-mediated growth under controlled electrochemical biasing led to syntheses of unusual morphology “microcups and microbowls/microlanters” of polypyrrole films. It was noticed that the density, shape, wall thickness, and caliber of polypyrrole microstructures can be regulated by controlling the process conditions. These results are unprecedented and can be extended to synthesize similar microstructures of other materials.

The authors gratefully acknowledge the SEM and AFM facilities housed in the Center for Applied Science and Engineering (CASE) at the University directed by Dr. R. Giedd and operated by Mr. Rishi Patel. Also, thanks to Mr. N. Smith for technical assistance. This research work is financially supported by the internal funds.

¹For a review please see S. Roth, W. Graupner, and P. McNeillis, *Acta Phys. Pol.* **87**, 699 (1995); J. S. Miller, *Adv. Magn. Reson.* **5**, 587 (1993).

²T. Fernández Otero and H. Jürgen Grande, in *Handbook of Conducting Polymers*, edited by T. A. Skotheim, R. L. Elsenbaumer, and J. R. Reynolds (Marcel Dekker, New York, 1998), Vol. I, Chap. 36, p. 1015.

³C. R. Martin, *Science* **266**, 1961 (1994).

⁴S. Cuenot, S. D.-Champagne, and B. Nysten, *Phys. Rev. Lett.* **85**, 1690 (2000).

⁵S. Shirator, S. Mori, and K. Ikeyaki, *Sens. Actuators B* **49**, 30 (1998).

⁶Z. Cai and C. R. Martin, *J. Am. Chem. Soc.* **111**, 4138 (1989).

⁷L. Qu, G. Shi, F. Chen, and J. Zhang, *Macromolecules* **36**, 1063 (2003).

⁸V. Bajpai, P. He, and L. Dai, *Adv. Funct. Mater.* **14**, 145 (2004).

⁹N. Balci, E. Bayramli, and L. Toppare, *J. Appl. Polym. Sci.* **64**, 667 (1997).

¹⁰Y. Yang and M. Shi, *J. Mater. Chem.* **11**, 2022 (2001).

¹¹S. M. Chia, A. C. A. Wan, C. H. Quek, H. Q. Mao, X. Xu, L. Shen, M. L. Ng, K. W. Leong, and H. Yu, *Biomaterials* **23**, 849 (2002).

¹²R. Kostj, D. Rakovi, S. A. Stepanyan, I. E. Davidova, and L. A. Gribov, *J. Chem. Phys.* **102**, 3104 (1995).

¹³C. M. Jenden, R. G. Davidson, and T. G. Turner, *Polymer* **34**, 1649 (1993); S. D. Champagne and P. Y. Stavauz, *Chem. Mater.* **11**, 829 (1999).